Progress of the X-Com project and PhD research - Report 2

Produced by:

John Atkinson, PhD Researcher, atkinsonj@bournemouth.ac.uk

Dr Luciana S. Esteves, Principal Academic, lesteves@bournemouth.ac.uk

Bournemouth University

Faculty of Science and Technology
Bournemouth University
Talbot Campus, Poole, Dorset, BH12 5BB, UK
Phone: +44 (0) 1202 9 62446

21st June 2017

CONTENTS

ABBREVIATIONS

Cefas	Centre for Environment, Fisheries and Aquaculture Science
DGPS	Differential Global Positioning System
DirP	Peak period direction (degrees true)
DWR	Datawell Waverider wave buoy
EA	Environment Agency
Hs	Significant wave height (metres)
Metocean	Meteorological and oceanographical
MSL	Mean Sea Level (metres)
ODN	Ordnance Datum Newlyn (metres)
RMSE	Root mean square error
SCDC	Suffolk Coastal District Council
SNR	Signal to Noise Ratio
X-Com	X-band radar and evidence-based Coastal Management decisions

Acknowledgement of Funding Sources

X-band radar and evidence-based coastal management decisions (X-Com) was a project funded by the Natural Environment Research Council (reference NE/M021564/1). X-Com partners and collaborators included: Bournemouth University (BU), National Oceanography Centre (NOC), Suffolk Coastal District Council (SCDC), Mott MacDonald, Cefas and residents of Thorpeness. The PhD studentship is co-funded by Bournemouth University, Suffolk Coastal District Council and Mott MacDonald.

1 Introduction

This document is the second quarterly report summarising the data collection and preliminary results of the PhD research undertaken in association with the X-Com project. The first progress report (submitted on 31st Jan 2017) presented an overview of data types and methods of data collection and analysis, which will not be repeated here. This report will present an update on the data collected and analysed so far and will focus on initial results on changes in beach topography.

The X-band radar system installed on the cliff top at the northern end of Thorpeness (Suffolk, UK) collected data between 16th September 2015 (the date of installation) and 19th April 2017 (the date of decommission). Figure 1 shows the radar data coverage and the progress of the raw data processing as of 20th May 2017; final raw data return for the radar deployment was 62.1% with 100% return since November 2016. The PhD research started on 24th January 2016 and is expected to be completed in three years.

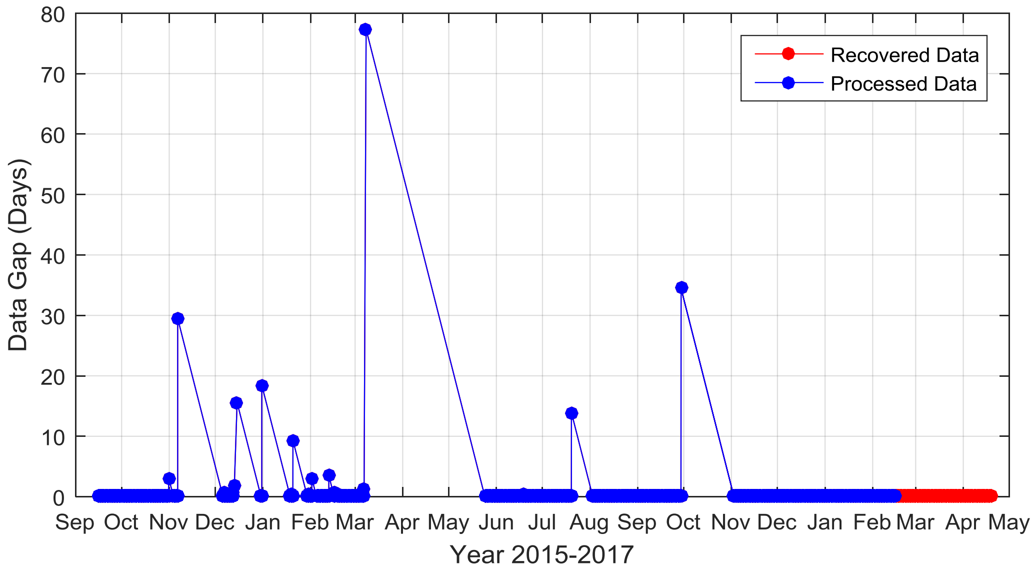

Figure 1. Radar data coverage and processing progress.

Section 2 of this report presents calibration of the radar wave heights used in volume change analysis. An updated analysis of meteorological and oceanographic conditions from the West Gabbard buoy is presented in Section 3 with summary statistics of both winter and annual wave data. Section 4 presents radar analysis of nearshore bathymetric changes seasonally and due to storm impact. Preliminary results from the analysis of fieldwork data to quantify beach change and cliff recession are presented in Sections 5 and 6 respectively. Section 7 outlines the next steps related to both data collection and analysis.

2 WAVE DATA CALIBRATION

Wave heights cannot be directly inferred from radar raw data due to non-linearity of the radar imaging mechanism (Borge *et al*. 1999). When wave measurements from another instrument are collected concomitant with radar imaging, a calibration method (Alpers & Hasselmann 1982) can be applied to adjust the wave height obtained from the radar. Calibration coefficients can be calculated using equation 1, where H_s is the calculated calibrated significant wave height, A is the intercept of the y axis and B the slope of the fit between Signal to Noise Ratio *(SNR)* and calibrated H_s.

$$H_s = A + B\sqrt{SNR} \tag{1}$$

The radar data recorded at Thorpeness was calibrated using the Cefas Sizewell Datawell Waverider (DWR) located approximately 1900 m north and 3500 m east of the radar position. Figure 2 shows the correlation between the calibrated wave radar data and the wave buoy measurements. The R^2 value of 0.74 and root mean square error (RMSE) of 0.25 m suggest reasonable accuracy of the radar for wave height based on comparison with other similar studies. Literature values applying the same method show accuracy of R^2 = 0.89 in deep (380 m) water (Borge *et al.,* 1999), Izquierdo & Guedes Soares (2005) and Carrasco *et al*. (2016) gave RMSE of 0.28 m and 0.24 m respectively but no R^2 value. In some cases, the error is not quantified or presented explicitly and instead refers to a 'high degree of correlation' (Reichert and Lund, 2007; Hessner *et al*., 2015).

A visual comparison of the time series of the calibrated radar data and wave measurements (Figure 3) shows that higher waves are underestimated by the radar, while small waves tend to be overestimated. This difference is a consequence of the poor fit of the linear regression (see Figure 2) for waves higher than 1.5 m due to the effect of data concentration towards smaller waves. Therefore, the calibration method will be revised to improve results.

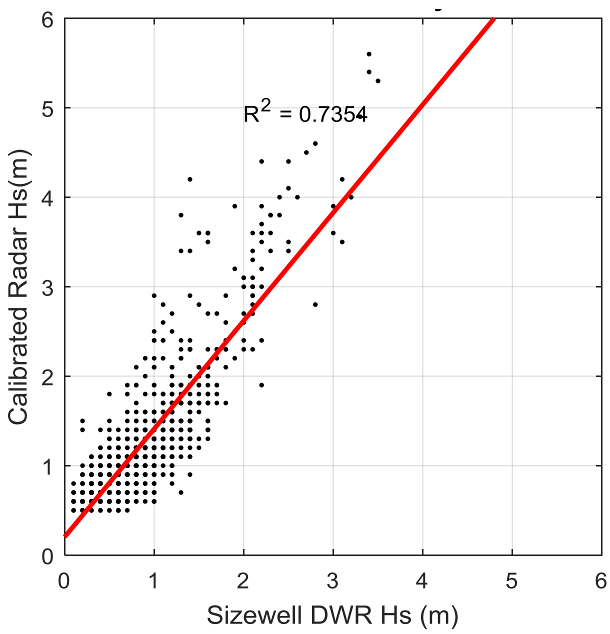

Figure 2. Correlation between the calibrated wave heights extracted from the radar data and measurements from the Sizewell DWR showing the resulting Pearson Correlation Coefficient squared (R^2).

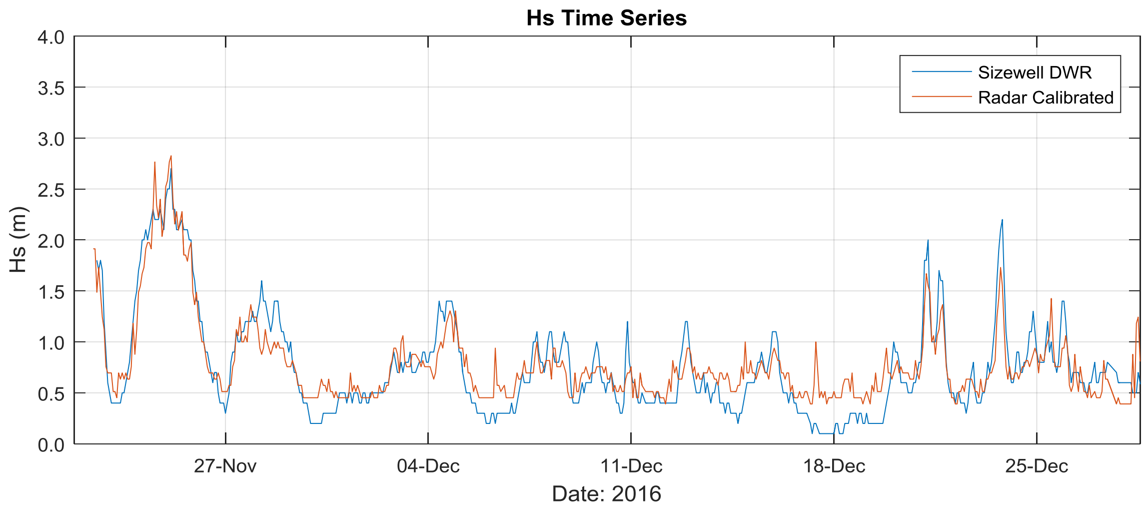

Figure 3. Time series of calibrated wave heights extracted from radar data and measurements by the Sizewell DWR for the period between 22nd Nov and 28th Dec 2016.

3 Wave Climate

To characterise the wave climate in the study area and its variability, measurements recorded by the West Gabbard Cefas Wavenet buoy (~40 km southwest of Thorpeness) were analysed. Using the wave buoy data, wave roses were produced for all waves (Figure 4a) and for wave heights exceeding 2.5 m (Figure 4b) for the two winters coinciding with radar data collection. Figure 4 indicates clearly that that southerly waves dominated over the 2015-2016 winter (81% of Hs > 2.5 m approached from the south), while northeasterly waves dominated in the 2016-2017 winter (60% of Hs > 2.5 m approaching from the northeast).

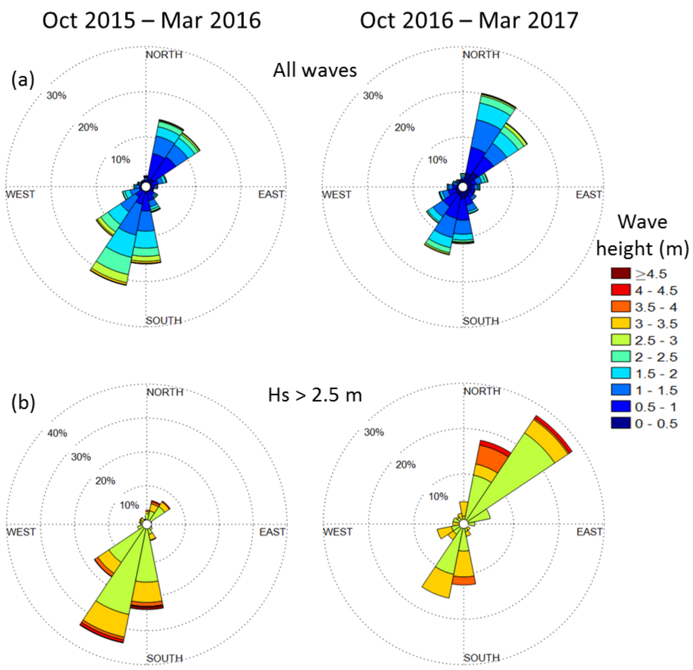

Figure 4 Wave roses of significant wave height measured by the West Gabbard wave buoy for all records (a) and Hs > 2.5 m (b) for the winters of 2015-16 and 2016-17.

It is important to understand the range of conditions that may be observed in the area so the data collected in this project can be placed into the longer-term context. Table 1 shows annual and winter (Oct-Mar) wave statistics of the data recorded by the West Gabbard wave buoy from 2006 to 2017. The variability in wave conditions between winters is evident in the mean and extreme wave heights and direction. It is worth noting that conditions in the 2015-16 winter are comparable to the 2013-14 winter, except for the extreme wave heights. The 2013-14 winter had the most extreme wave conditions recorded by the West Gabbard wave buoy, with the highest 5% of the waves (the 95 percentile) showing Hs > 2.93 m. In the 2015-16 winter, this threshold was considerably lower (Hs > 2.62 m), while the mean Hs was very similar in both winters (1.41 and 1.42 m). In terms of wave direction, conditions in the 2016-17 winter were similar to the 2009-10 winter, however mean and extreme wave heights were considerably lower in 2016-17 (see Table 1).

Table 1. Annual and winter (October-March) wave statistics of data recorded by the West Gabbard wave buoy.

	Significant Wave Height (m)			**Direction**				
Year	**95%ile**	**Max**	**Mean**	**Peak Hs (°)**	**N (%)**	**S (%)**	**Hs>2.5 N (%)**	**Hs>2.5 S (%)**
2006	2.32	4.09	1.09	000	50.37	49.63	15.07	84.93
2007	2.23	4.09	1.13	186	55.76	44.24	55.92	44.08
2008	2.41	5.25	1.14	180	47.54	52.46	35.77	64.23
2009	2.23	5.06	1.04	028	52.64	47.36	49.81	50.19
2010	2.32	4.55	1.06	034	63.30	36.70	78.21	21.79
2011	2.14	4.09	1.05	180	42.93	57.07	18.08	81.92
2012	2.23	4.24	1.05	039	48.18	51.82	45.52	54.48
2013	2.51	5.06	1.12	186	55.82	44.18	56.94	43.06
2014	2.32	4.39	1.10	191	49.12	50.88	19.53	80.47
2015	2.33	4.42	1.11	028	45.35	54.65	16.64	83.36
2016	2.37	4.83	1.11	201	49.03	50.97	44.28	55.72
Winter								
2006-07	2.61	4.09	1.36	0	37.97	62.03	25.91	74.09
2007-08	2.61	5.25	1.33	180	45.39	54.61	28.75	71.25
2008-09	2.41	3.94	0.97	174	59.23	40.77	43.16	56.84
2009-10	2.71	5.06	1.30	28	50.65	49.35	61.55	38.45
2010-11	2.41	4.55	1.22	34	58.93	41.07	59.94	40.06
2011-12	2.32	3.94	1.14	186	41.09	58.91	40.96	59.04
2012-13	2.61	4.09	1.33	219	51.43	48.57	61.61	38.39
2013-14	2.93	5.06	1.42	186	33.36	66.64	15.64	84.36
2014-15	2.42	3.89	1.28	170	42.87	57.13	33.43	66.57
2015-16	2.62	4.83	1.41	201	36.36	63.64	18.77	81.23
2016-17	2.33	4.18	1.15	24	48.85	51.15	60.14	39.86

4 NEARSHORE CHANGES

Radar data allows analysis of changes in bathymetry in a range of temporal scales. The previous report presented preliminary results of seasonal changes and illustrated the variation in bathymetric changes associated with two storm events. This report will present further analysis on seasonal and shorter-term bathymetric changes and initial results from an assessment of change in sediment volume.

4.1 LONGER-TERM CHANGES IN BATHYMETRY AND SEDIMENT VOLUME

To understand the variability in nearshore bathymetry at a seasonal scale, data analysis focused on identifying the maximum and minimum nearshore depths measured between September 2015 and November 2016. The baseline used to estimate sediment volume changes was defined as the deepest mean depth observed in the period within the radar view area. It is assumed that at its deepest state the area would have the least amount of sediment. The deepest mean depth was observed in November 2016 and this was considered the baseline condition (0 m^3) from which to calculate minimum, mean and maximum sediment volume changes. Table 2 shows the estimated minimum, maximum and mean sediment volume gained in each month and season in relation to the baseline (November 2016) within the 3.3 km^2 study area and respective data return in percentage of time. Low data return in the periods March – May 2016 and October 2016 was due to radar technical problems.

Table 2. Maximum, mean and minimum volume monthly and seasonally from September 2015 to November 2016 extracted from X-band radar data with corresponding data return.

Time period	Volume (m^3)			Valid Data Return (%)
	Max volume	**Mean volume**	**Min volume**	
Sep 15	112562	85805	76262	97
Oct 15	101364	65221	44717	99
Nov 15	88712	54181	41918	9
Dec 15	48737	31424	15840	21
Jan 16	24178	20039	16322	7
Feb 16	44614	24747	7526	65
Mar 16	36686	32968	30545	18
Apr 16	-	-	-	0
May 16	46248	39152	33932	24
Jun 16	88642	62292	35831	99
Jul 16	85394	49309	31869	59
Aug 16	103706	61455	47431	94
Sep 16	66797	56052	34863	93
Oct 16	-	-	-	0
Nov 16	58675	35247	0	94
Sep-Nov 15 (Autumn)	112562	68757	41918	60
Dec 15-Feb 16 (Winter)	48737	25923	7526	30
Mar-May 16 (Spring)	46248	36457	30545	14
Jun-Aug 16 (Summer)	103706	58881	31869	84
Sep-Nov 16 (Autumn)	66797	47513	0	62

Figure 5 shows the maximum sediment volume gained in relation to the baseline and the maximum volume change in each month and season. The maximum volume change refers to the difference between the maximum and minimum volume observed in each month or season and does not reflect the net change in that period. Data shown in Table 2 and Figure 5 suggest that sediment volumes are largest in the summer and decrease throughout the autumn to reach minimum values in the winter. Interestingly, it seems that sediment mobility (indicated as the maximum volume change) is also highest in the summer and autumn months and changes are less pronounced over the winter and spring (Figure 5). This observation needs to be considered carefully as during the winter months in 2015 data return was low. The volume changes are indicated here to enable relative comparison of sediment mobility across months and seasons and do not refer to erosion or deposition. Erosion and deposition trends vary spatially within the study area (see Figure 6 and Figure 7) and results from this analysis will be presented in future reports.

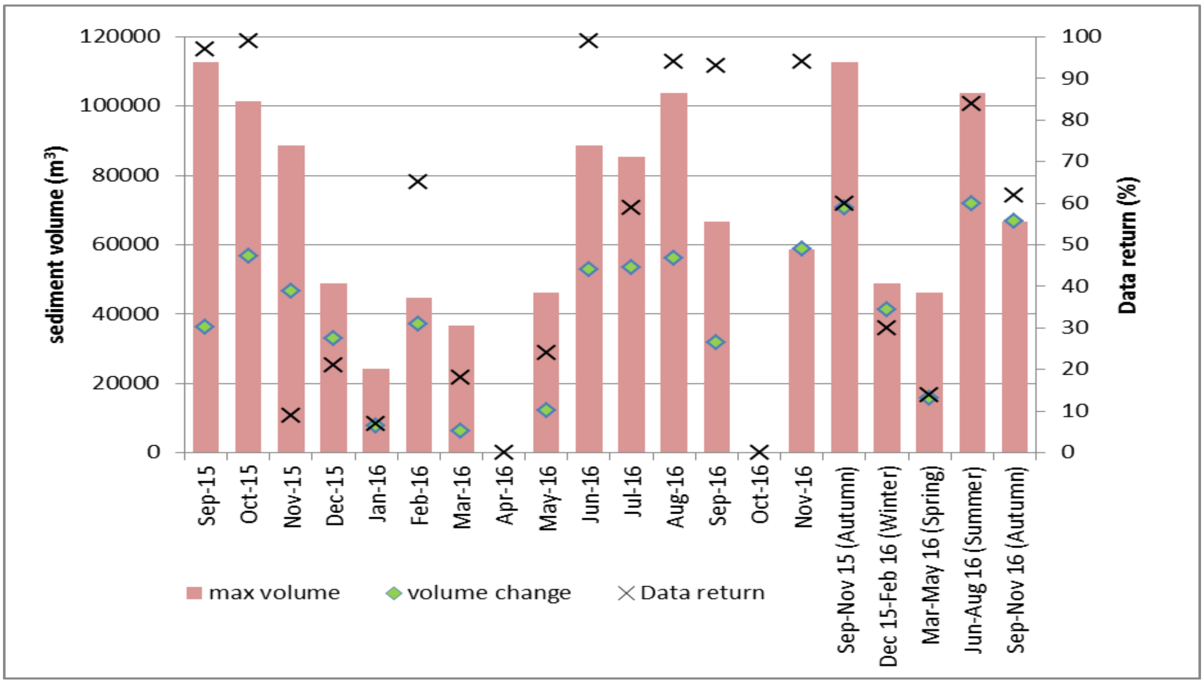

Figure 5. Maximum volume of sediment gained in relation to the baseline (November 2016), maximum volume change in each month and season and respective data return.

Figure 6a shows bathymetric contours derived from radar data obtained in 30th September 2015, 9th February, 19th August and 26th November 2016 to illustrate seasonal variations. This figure shows a large shallower area (depth<5 m ODN) extending from the SW in September 2015 and August 2016, which is not evident in February and November 2016. The changes in bathymetry between the dates shown in Figure 6a are displayed in Figure 6b. The radar data suggests considerable bathymetry changes reaching 3-4 m within the nearshore (Figure 6). These changes seem to indicate the development of an oblique bar in the spring and summer (accretion from February 2016 to August 2016) and its erosion in the autumn and winter (erosion from September 2015 to February 2016 and from August 2016 to November 2016). Magnitudes of change are reduced away from this area and can be minimal at the north and south of the study site. The orientation and position of the 'bar' and the areas of largest changes seem to follow the Coralline Crag ridge present in the study area. It is possible to infer that the underlying geology has an important effect on the morphology and evolution of nearshore sedimentary features.

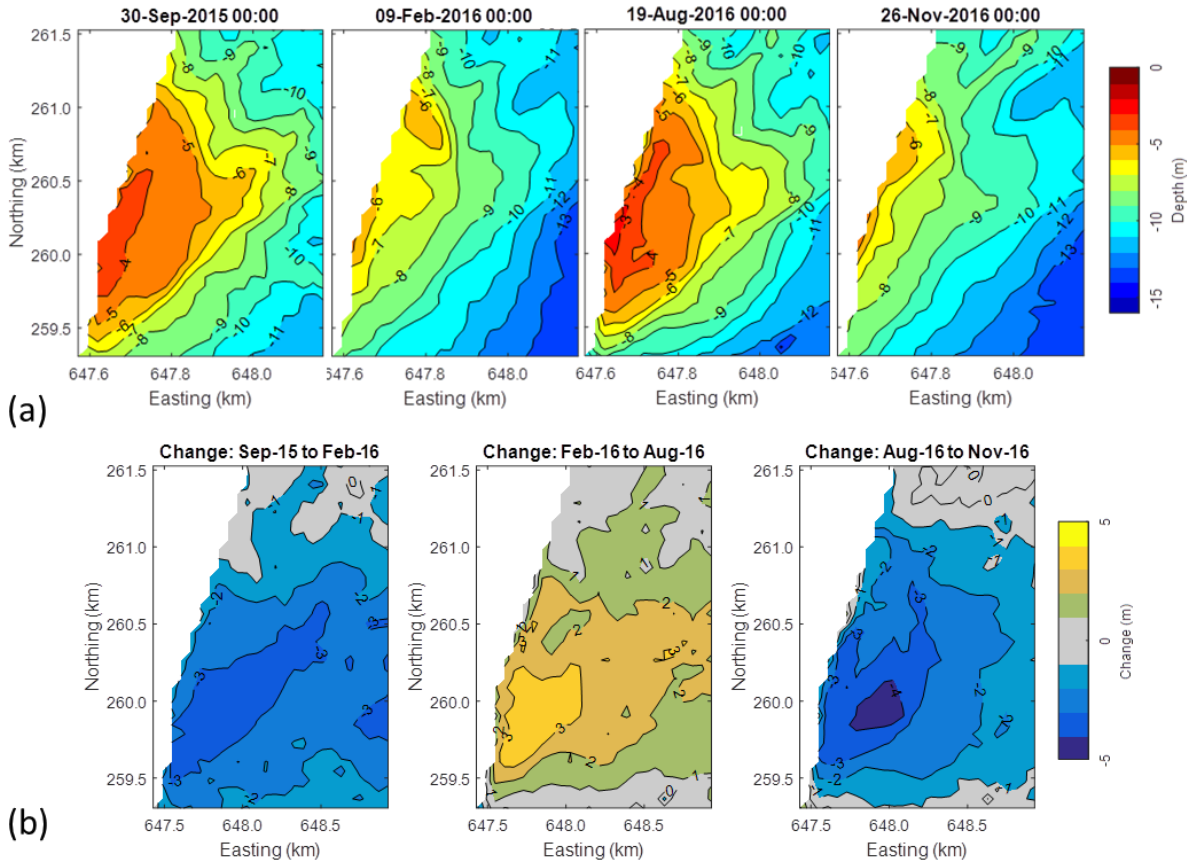

Figure 6. Radar derived bathymetric contours at four selected dates (a) and respective changes (b).

To further understand the seasonal changes shown in Figure 6, depth was extracted along two transects (T1 and T2), which are extensions of EA beach profiles. Figure 7 shows the bathymetric profiles for the four dates shown in Figure 6 and the standard deviation at each pixel calculated based on all data from September 2015 to November 2016. The largest changes in bathymetry are observed in the nearshore of T2 (cross-shore distance between 0-500 m). In both transects, a clear seasonal variation is observed, with accreted (shallower) profiles at the end of summer (September 2015 and August 2016) and eroded (deeper) profiles at the end of Autumn (November 2016). Between November and February 2016, changes are small, mainly accretion, except in the nearshore of T1 where erosion was observed. These results support the interpretation of data shown in Figure 5 that sediment volumes are largest in September (reflecting accreted conditions) and reduce throughout the autumn, with smallest volumes (eroded conditions) in the winter months, when sediment mobility (volume change) tends to be minimal.

Figure 7 shows that in T2 summer accretion of up to 4 m is pronounced in the nearshore (up to 500 m offshore), in T1 accretion (~3 m) is more pronounced further offshore (700-1100 m). This difference reflects the SW-NE orientation of the oblique bar, which seems to reduce in size northwards. Particularly along T2, the seasonal signal is striking, with 'summer' and 'winter' profiles showing very similar shape and depths. Along both transects, the evident increase in slope at 500-600 m distance offshore may be an effect of the underlying geology, which is likely to control the position of the oblique bar.

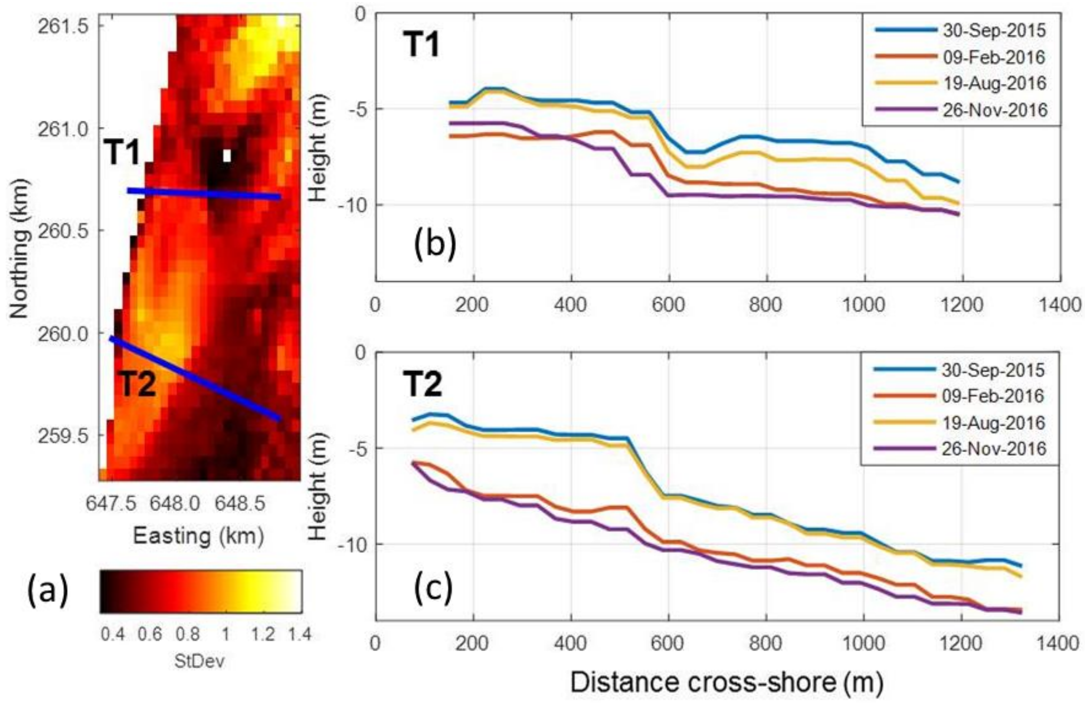

Figure 7. Standard deviation of each pixel between 30th September 2015 and 26th November 2016 (a) and the radar derived depth along the T1 (b) and T2 (c).

4.2 Shorter term changes in bathymetry

Periods of largest change in the short term were identified as the highest standard deviation in the depth at each pixel within any 7-day period. An algorithm was used to identify periods in which standard deviation exceeded 0.2 m in 7 consecutive days. After data quality checks, volume changes were calculated for each pixel and the metocean conditions were characterized to identify whether the changes resulted from: (a) single high energy significant event; (b) clustered events; or (c) persistent conditions. Storm events here were identified using the thresholds of Hs ≥1.5 m and duration >6 hours. To quantify the relative energy of these storm events the 'storm power index' (S_{pi}) was calculated using equation 2 (Dissanayake et al., 2015), where D = duration above threshold, H = significant wave height:

$$S_{pi} = \sum_{i=1}^{n} (\Delta D \times \Delta H_i^2) \quad (2)$$

The largest recorded changes were observed in the period 20th to 27th November 2016, when a cluster of three individual storms was recorded (Figure 8). The first two storms approached from the SE and the third storm approached from the NE. Table 3 presents the start and end times of the three clustered storms and their respective peak Hs, Spi and sediment volume changes within the radar view (total m^3 and total m^3/hour). Storm 1 had the lowest Spi and resulted in the largest total volume change and change per hour. Storms 2 and 3 lasted longer, had Spi higher than storm 1 but resulted in less volume change. However, volume changes caused by each storm were spatially variable (Figure 9).

Figure 9 shows the standard deviation and the depth profiles along transects T1 and T2 for four selected dates during the period of the clustered storms of 20th – 27th November 2016. Storm 1 (20th – 21st November) approached from the SE and caused erosion across both profiles, which was more evenly distributed from the nearshore up to 800 m offshore along T2 and more pronounced (>1 m) between 800-1200 m offshore in along T1. Storm 2 (22nd – 23rd November) caused relatively little impact on T1 whereas erosion was observed along T2 between 100 m and 600 m offshore (although of lower magnitude than storm 2). Storm 3 (24th – 26th November) approached from the NE and had greater impact (erosion exceeding 1 m) in the nearshore of T1 (between 300 and 600 m) and little change elsewhere. These results suggest that greater impact in the southern and northern part of the study area are caused by storms approaching from SE and NE, respectively. Further analyses are required to identify the influence of longshore and cross-shore sediment transport and interactions with the underlying geology on spatial variations in nearshore change.

Table 3. Storm timings, storm power index (Spi) and associated sediment volume changes in the nearshore of the study area for three clustered storms in November 2016

Storm	Start Time	End Time	S_{pi}	Volume Change Radar View (m^3)	Volume changes (m^3/h)
1	20-Nov-2016 02:00	20-Nov-2016 13:30	59.39	-20536	1785.74
2	21-Nov-2016 23:30	22-Nov-2016 13:00	86.13	-9737	721.26
3	24-Nov-2016 02:30	25-Nov-2016 20:30	200.57	-10823	257.69

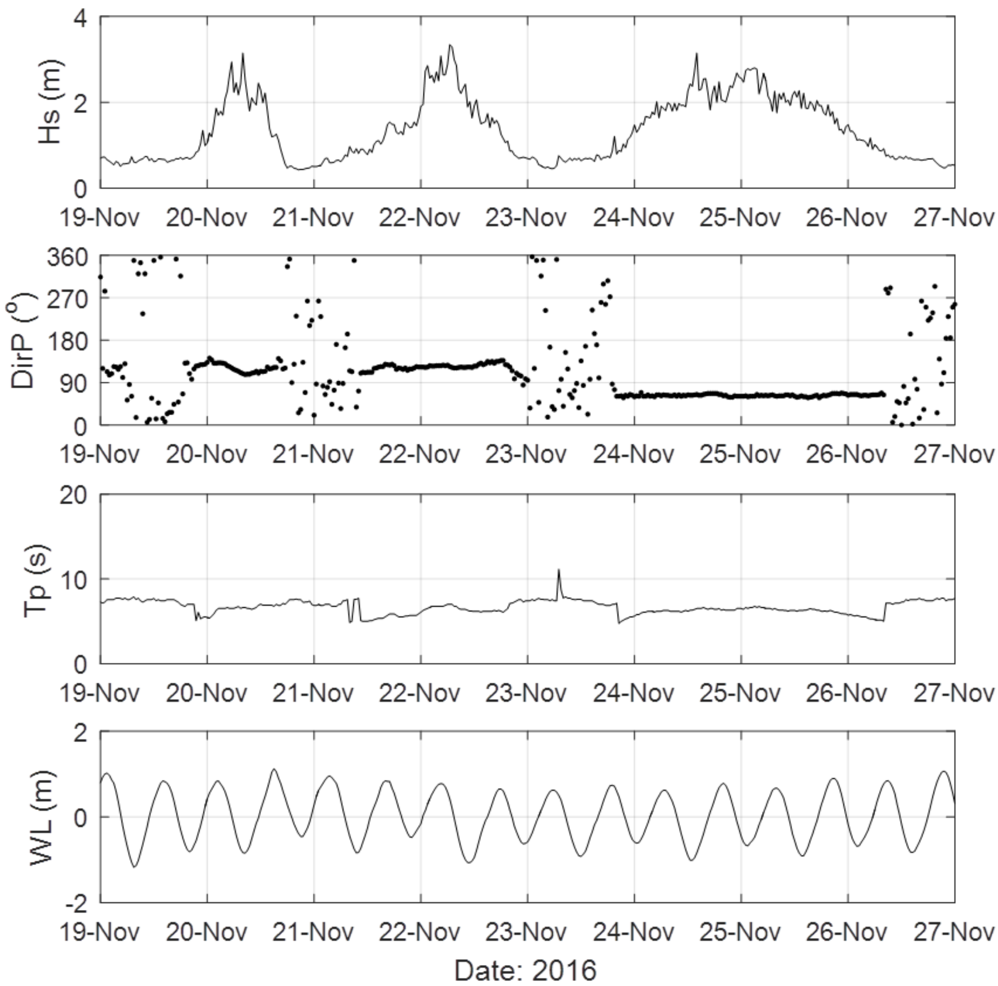

Figure 8. From top to bottom the panels show radar-derived significant wave height (Hs), peak period direction (DirP), peak period (Tp) and water level (WL) in relation to mean sea level (MSL) for the period 19th to 27th November 2016.

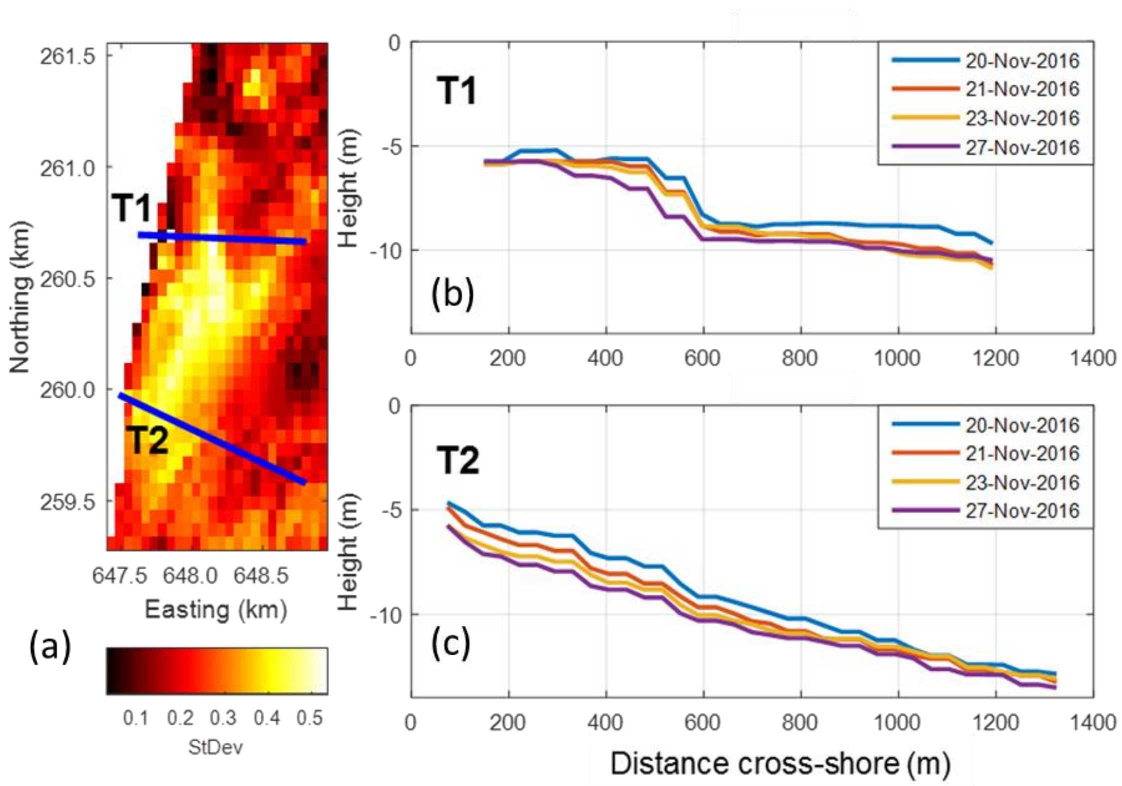

Figure 9. Standard deviation of depth values (a) and depth profiles along transects T1 (b) and T2 (c) for four selected dates during the period of the clustered storms of 20th – 27th Nov 2016.

5 Changes in Beach Topography

Changes in beach topography can be quantified through analysis of field work data. Figure 10 shows the spatial coverage of the laser scans and DGPS surveys undertaken to date. This report presents preliminary results of beach change based on the laserscan surveys undertaken on 3rd August 2016, 22nd October 2016, 6th December 2016, 18th January 2017, 13th February 2017 and 21st March 2017 they should be considered with caution until further quality checks are performed. Beach elevation changes were analysed at spatial resolution of 0.25 m and shown in more detail at selected cross-shore profiles (Figure 11-16). Figures 11-16 also show summary statistics of wave conditions for the respective periods and wave roses for waves Hs>1m. A detailed description of methods, volume change calculations and confirmation of results will be presented in the next report.

Net beach changes between 3rd August 2016 and 21st March 2017 (Figure 11) are spatially variable, showing erosion dominating north of P2, accretion in the upper and lower beach between P2 and P3 and a more stable beach around P4. The most noticeable change in the period is the cliff retreat of around 5.3 m and flattening of the beach observed north of the radar (evident in P1, Figure 11). The dynamic nature of the gravel ridges (changes in cross-shore position and elevation) is observed in P3 and the stable back beach observed in P4. During this period waves are dominant from NE (particularly the highest waves) and ENE, explaining the largest changes observed in the north of the study area. Figure 12 to Figure 16 indicate that beach changes are variable through time with largest changes occurring between 22nd October 2016 and 18th January 2017.

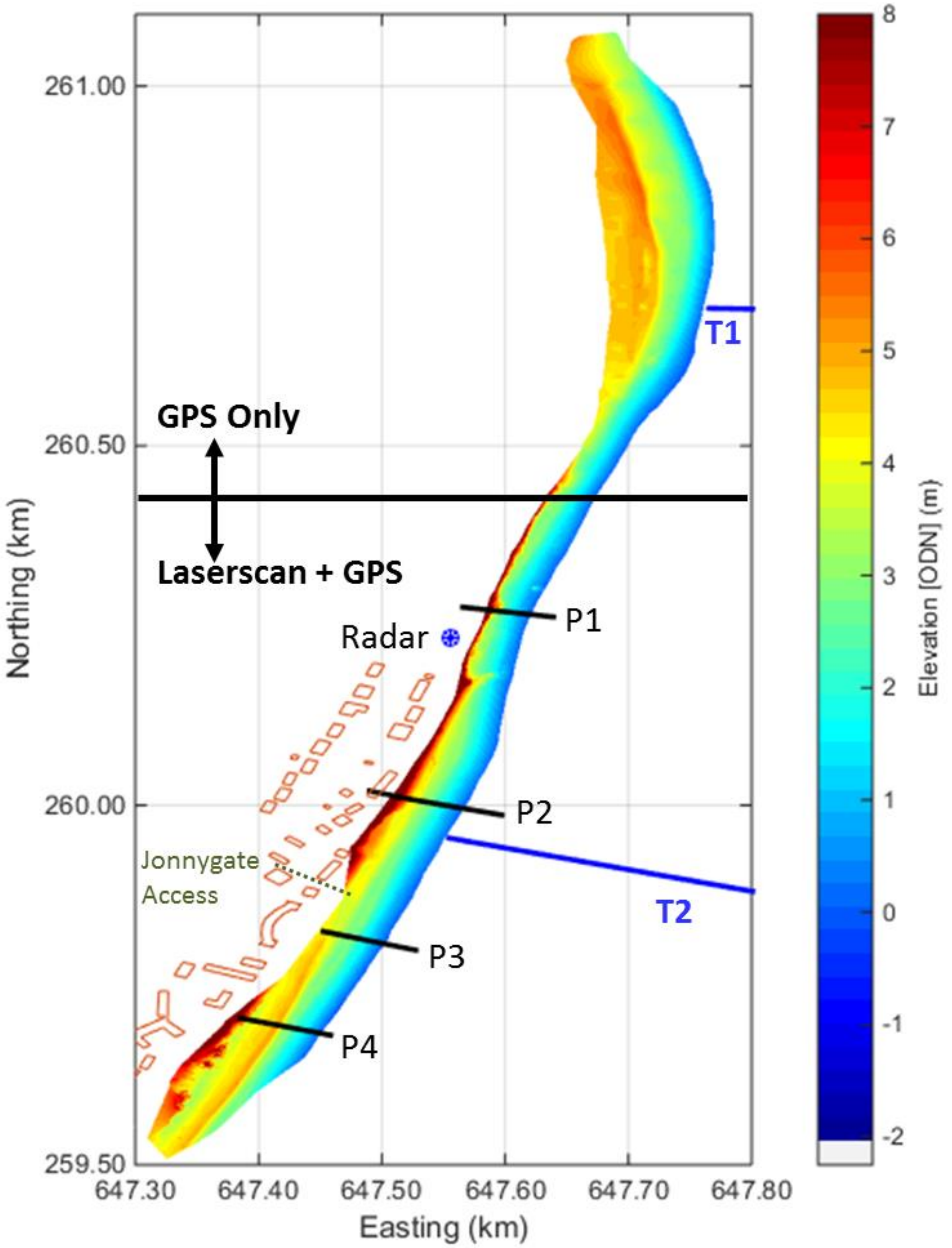

Figure 10. Beach and cliff elevations based on laser scan and DGPS data collected on 13th Feb 2017. P1-4 indicates the location of cross-shore profiles, T1 and T2 the offshore transects, near beach residencies and Jonnygate access indicated.

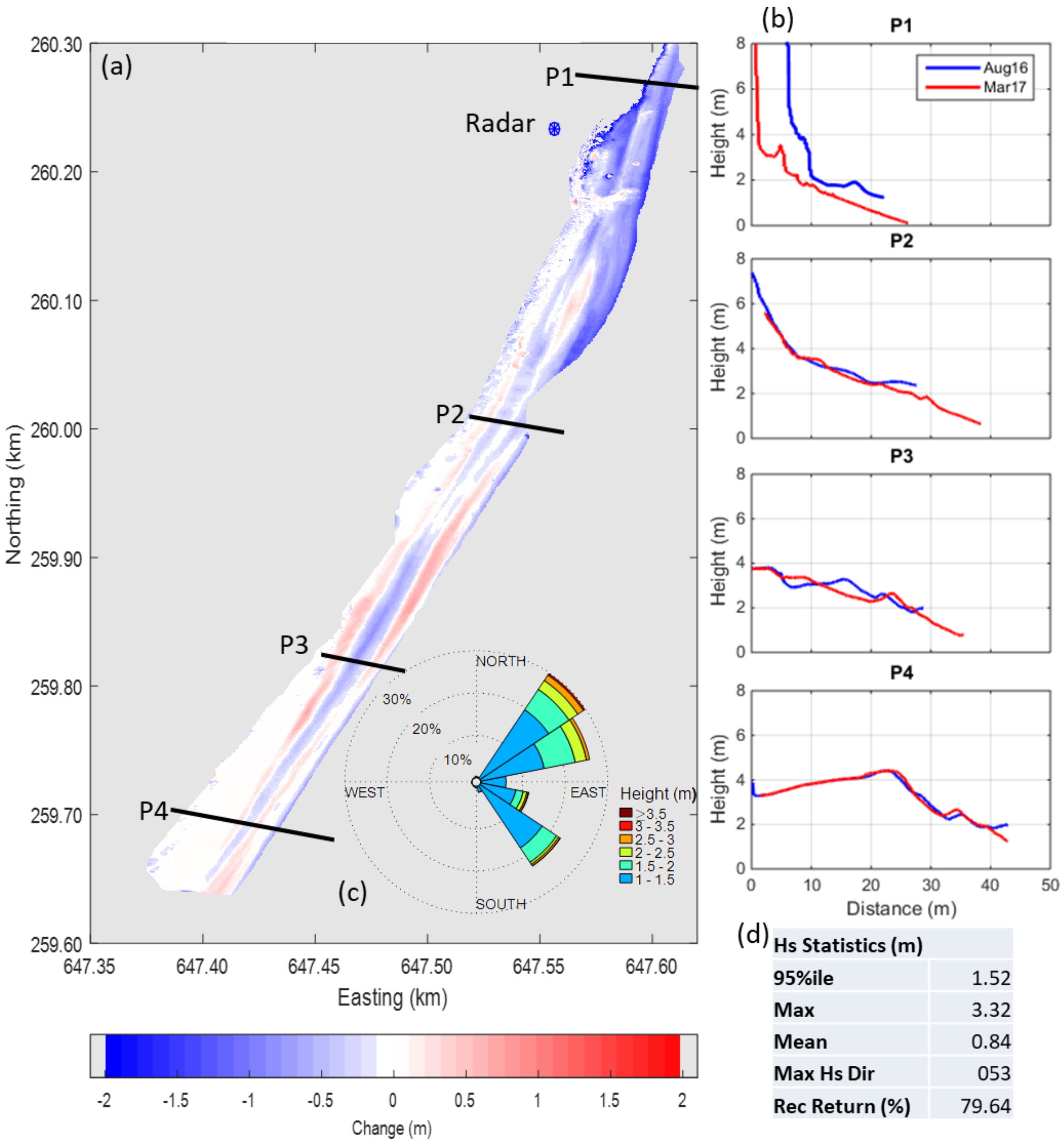

Hs Statistics (m)	
95%ile	1.52
Max	3.32
Mean	0.84
Max Hs Dir	053
Rec Return (%)	79.64

Figure 11. Changes in beach elevation and radar derived wave parameters between 3rd Aug 2016 and 21st Mar 2017 (a) spatial change and profile locations; (b) topography along selected profiles P1 – P4; (c) wave roses of peak direction for Hs>1 m; and (d) summary statistics of wave conditions in the period and percentage of data return for radar derived wave records.

Between 3rd August 2016 and 22nd October 2016 (Figure 12) changes in beach elevation are relatively small (<0.8 m) and dominated by accretion and berm formation south of P1. Wave conditions during this period were of relative low energy (95th percentile Hs=1.11 m; mean Hs= 0.76 m) and approaching dominantly from the SE. The largest changes in beach change were observed as an accretion at the cliff toe in P1. Further analysis is required to ascertain whether this accretion was due to sandy talus created by cliff face failure or gravel accretion due to longshore or cross-shore transport.

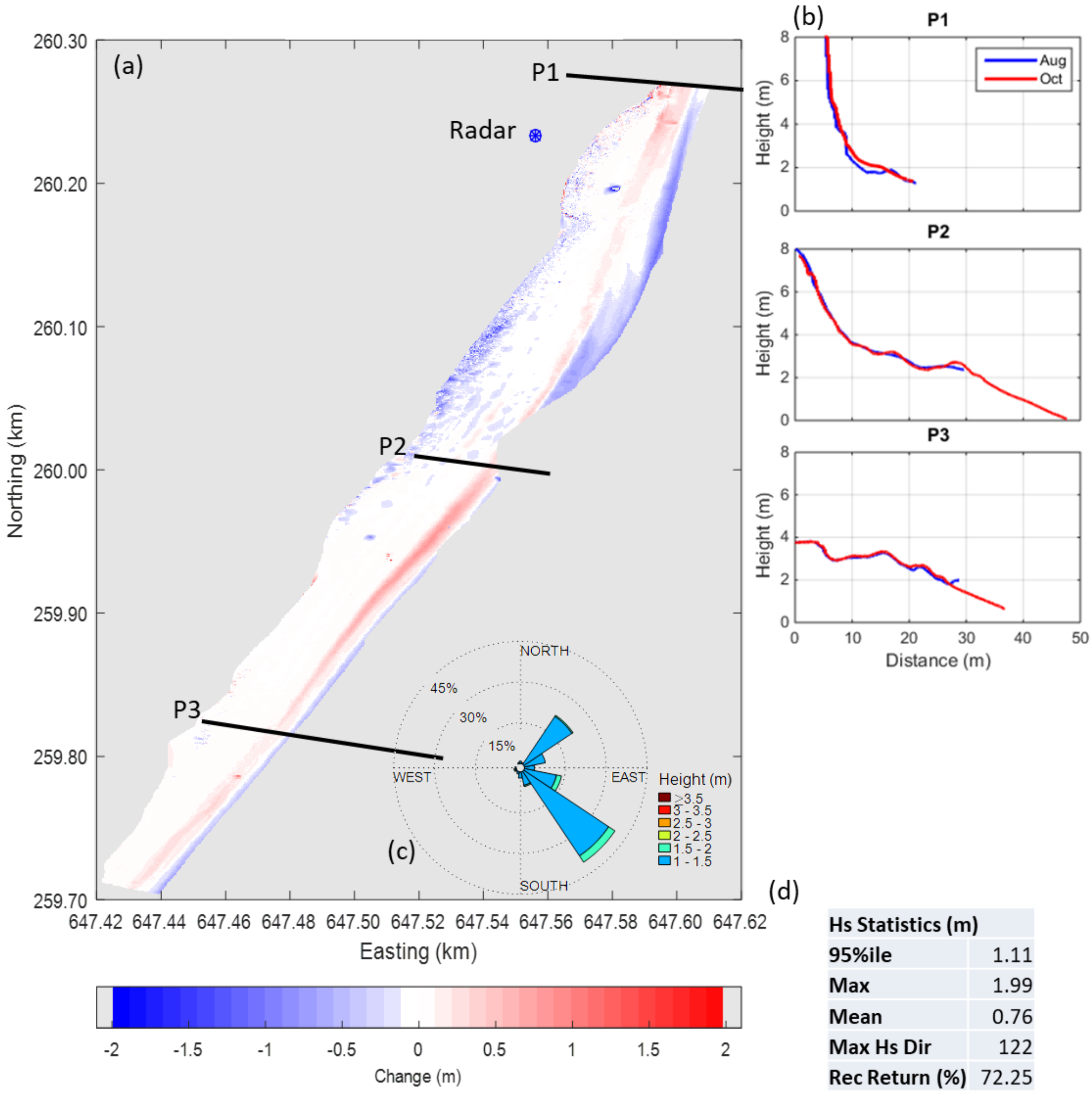

Hs Statistics (m)	
95%ile	1.11
Max	1.99
Mean	0.76
Max Hs Dir	122
Rec Return (%)	72.25

Figure 12. Changes in beach elevation and radar derived wave parameters between 3rd Aug 2016 and 22nd Oct 2016 ((a) spatial change and profile locations; (b) topography along selected profiles P1 – P3; (c) wave roses of peak direction for Hs>1 m; and (d) summary statistics of wave conditions in the period and percentage of data return for radar derived wave records.

Between 22nd October and 6th December 2016 (Figure 13) erosion is observed across the beach in the north of the scanned area, with cliff recession of 2.5 m at the cliff toe. Further south (P2 and P3), erosion mainly reflects berm lowering (-0.8 m at 15-25 m cross-shore) with an accretion (0.3 m) at the lower beach (25-45 m cross-shore) as shown in P3. This period showed the highest waves in the data analysed in this report (95th percentile Hs=2.2 m; mean Hs= 0.98 m) dominantly approaching from ENE and NE, contrasting with the previous period of quiescent wave conditions approaching from the SE.

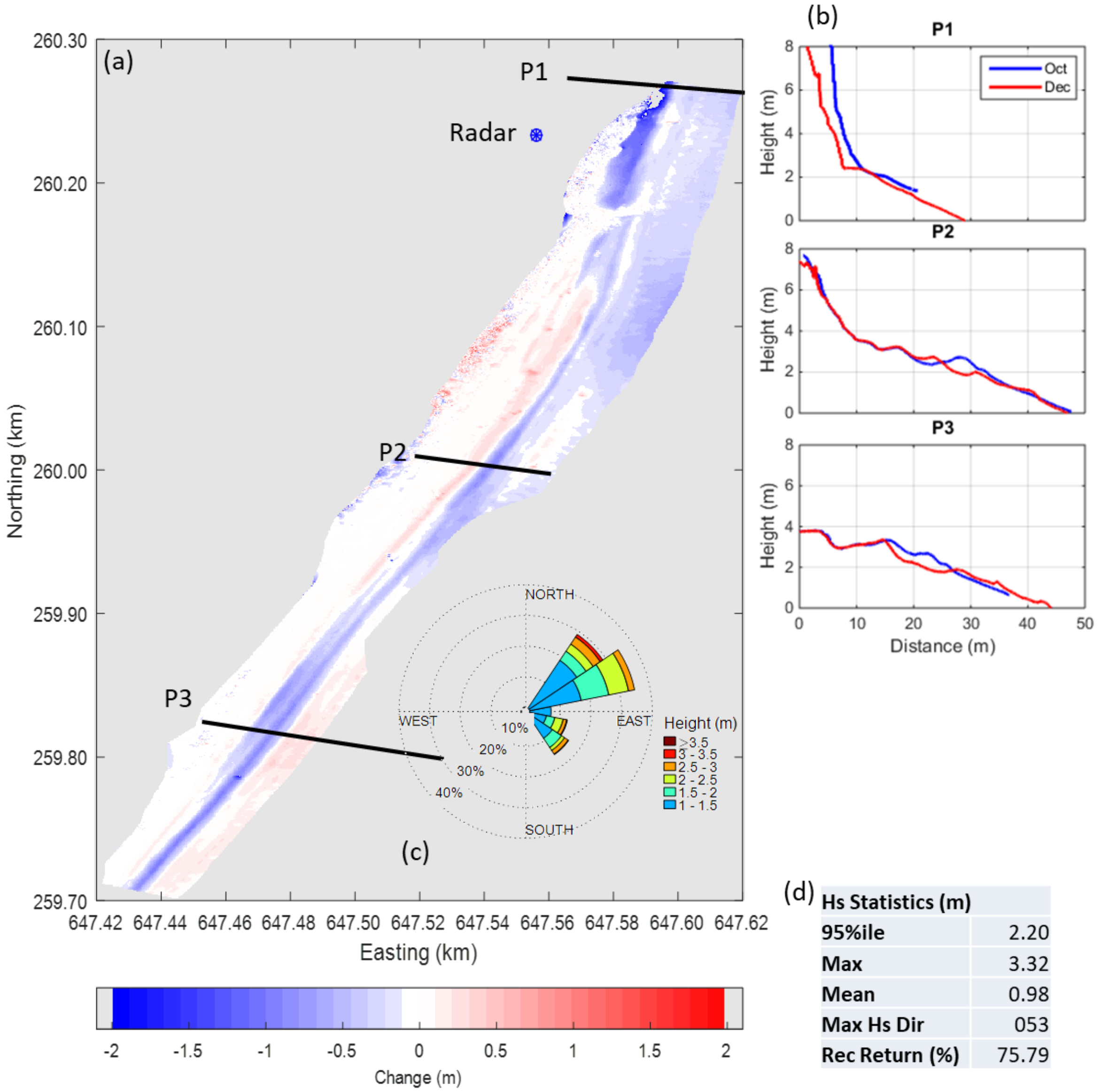

Hs Statistics (m)	
95%ile	2.20
Max	3.32
Mean	0.98
Max Hs Dir	053
Rec Return (%)	75.79

Figure 13. Changes in beach elevation and radar derived wave parameters between 22nd Oct 2016 and 06th Dec 2016. (a) spatial change and profile locations; (b) topography along selected profiles P1 – P3; (c) wave roses of peak direction for Hs>1 m; and (d) summary statistics of wave conditions in the period and percentage of data return for radar derived wave records.

Relative high energy wave conditions continued in the period 6th December 2016 to 18th January 2017 with a radar derived peak Hs=2.90 m coinciding with a storm surge of 1.56 m recorded at Lowestoft on the 13th January. Peak Hs=3.12 m occurred on the 4th January and waves were dominant from the NE (particularly Hs>2 m). The impact of these events enhanced the cliff toe retreat (reaching 4.8 m in P1) in the north of the study area (Figure 14), probably as a result of higher water levels due to the storm surge. P2 and P3 show a general flattening and removal of beach features (up to 0.3 and 0.6 m respectively). On the other hand, the beach around P4 remains relatively stable, with only minimal lowering (~0.2 m) of the beach face.

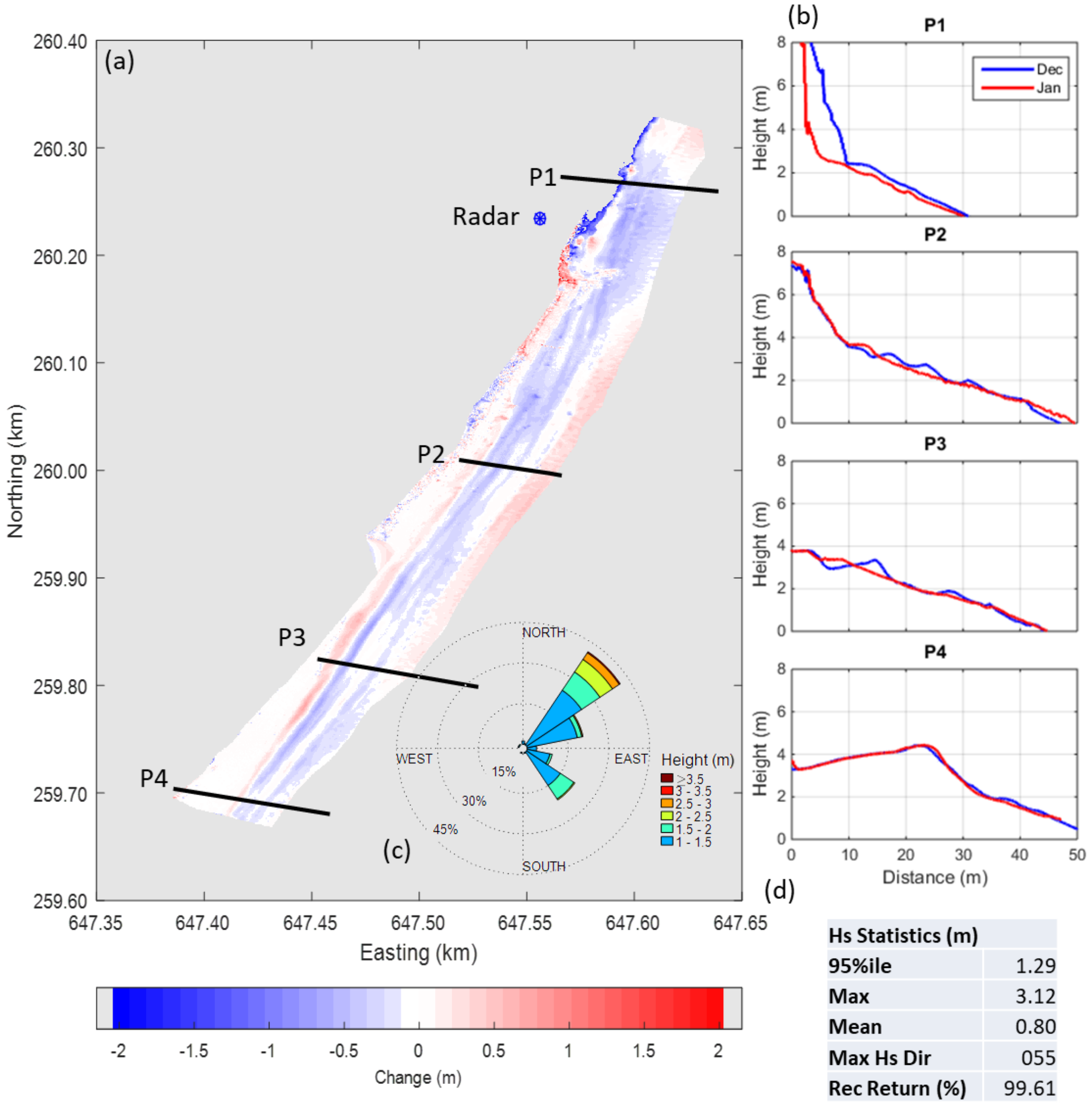

Hs Statistics (m)	
95%ile	1.29
Max	3.12
Mean	0.80
Max Hs Dir	055
Rec Return (%)	99.61

Figure 14. Changes in beach elevation and radar derived wave parameters between 06th Dec 2016 and 18th Jan 2017. (a) spatial change and profile locations; (b) topography along selected profiles P1 – P4; (c) wave roses of peak direction for Hs>1 m; and (d) summary statistics of wave conditions in the period and percentage of data return for radar derived wave records.

Wave conditions in the period 18th January – 13th February 2017 (Figure 15) continued to approach dominantly from the NE but were of higher energy (95th percentile Hs=1.64 m; mean Hs= 0.92 m) than in the previous period (6th December 2016 – 18th January 2017, Figure 14). However, beach changes were relatively small despite the intensification of the wave conditions. A slight steepening of the cliff face in the north of the study area (P1, Figure 15) seems to have provided sediment (sand) for accretion of the adjacent beach, while berm formation and a stable back beach is observed in south of the radar suggesting onshore sediment movement (P2 to P4, Figure 15). The lesser impact despite the intensification of wave conditions might be due to a combination of factors, which need to be investigated further, such as: the cliff/beach system was already at a very retreated state and water levels did not allow wave attach at the upper beach and/or erosion elsewhere has supplied sediment to compensate for sediment eroded from the area.

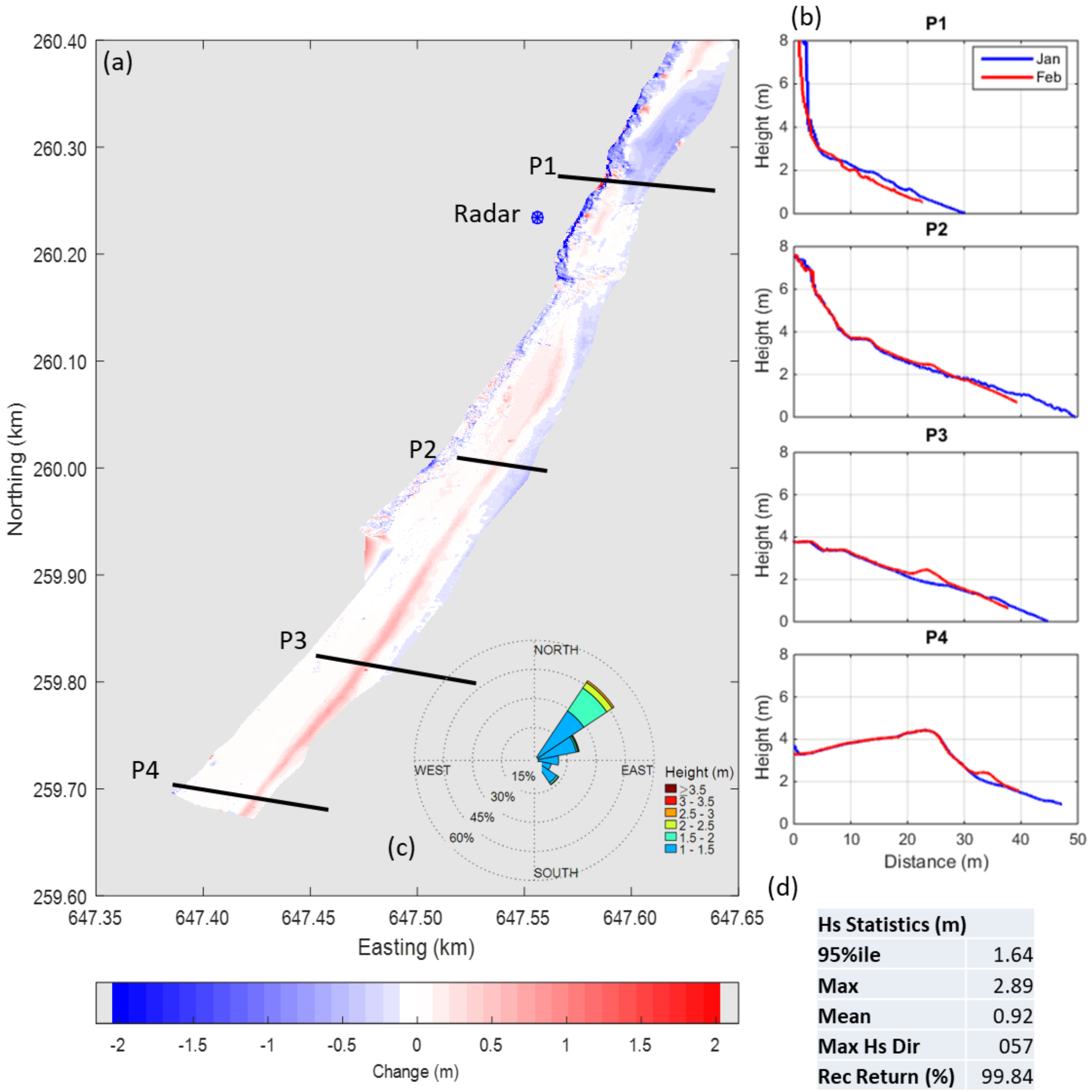

Hs Statistics (m)	
95%ile	1.64
Max	2.89
Mean	0.92
Max Hs Dir	057
Rec Return (%)	99.84

Figure 15. Changes in beach elevation and radar derived wave parameters between 18th Jan 2017 and 13th Feb 2017. (a) spatial change and profile locations; (b) topography along selected profiles P1 – P4; (c) wave roses of peak direction for Hs>1 m; and (d) summary statistics of wave conditions in the period and percentage of data return for radar derived wave records.

From 13th February to 21st March 2017 wave conditions were receding and less intense than in previous periods and bi-directional, approaching from the ENE and SE. Beach changes are even less prominent than the ones observed previously, with areas of erosion and accretion intercalating both cross-shore (lowering of the upper beach and accretion of the lower beach or vice-versa) with increased stability towards the south of the study area (Figure 16).

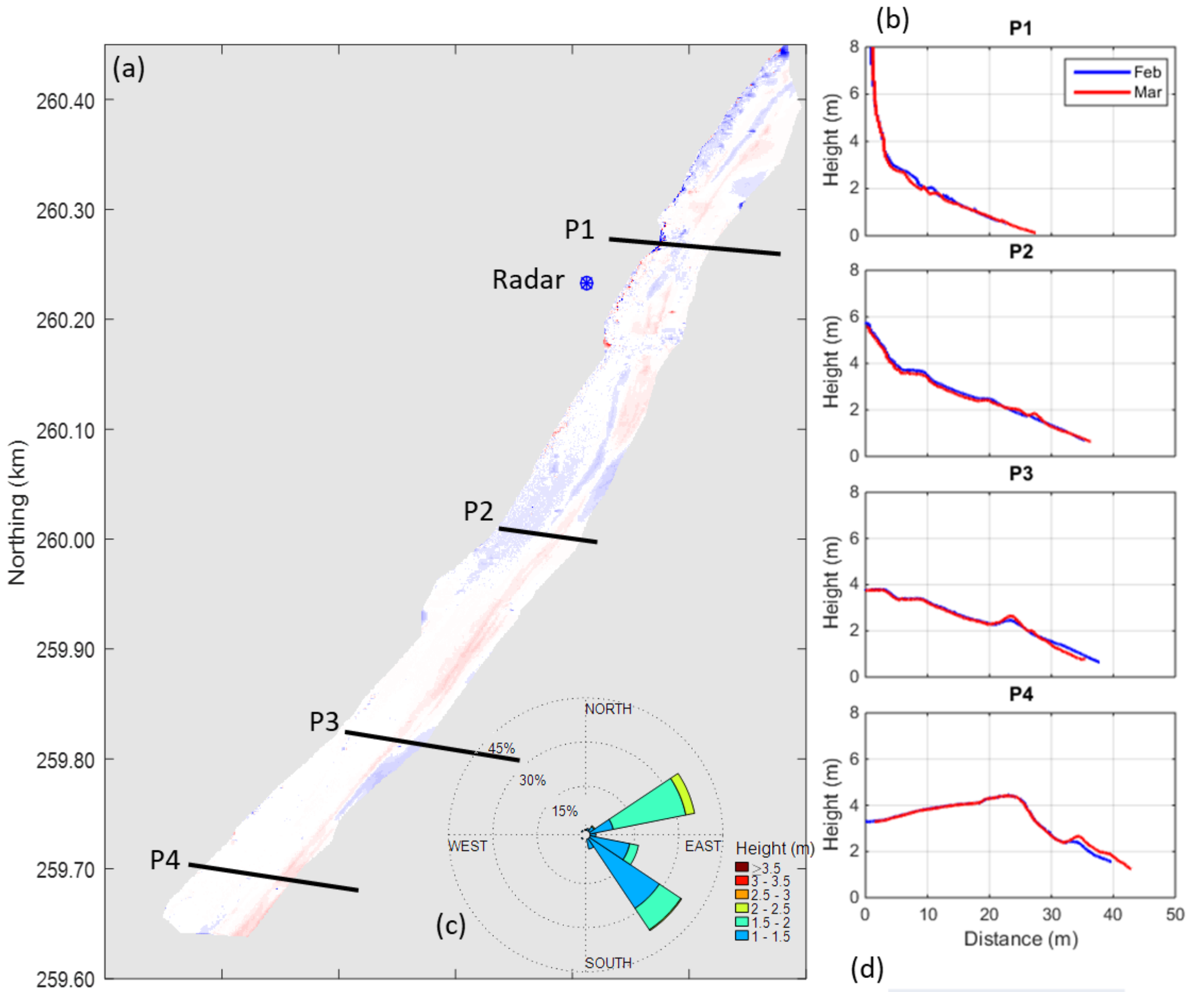

Hs Statistics (m)	
95%ile	1.61
Max	2.31
Mean	0.82
Max Hs Dir	062
Rec Return (%)	99.88

Figure 16. Changes in beach elevation and radar derived wave parameters between 13th Feb 2017 and 21st Mar 2017. (a) spatial change and profile locations; (b) topography along selected profiles P1 – P4; (c) wave roses of peak direction for Hs>1 m; and (d) summary statistics of wave conditions in the period and percentage of data return for radar derived wave records.

6 Cliff Recession

This report presents preliminary results of cliff recession over the winter 2016-2017 based on the surveys undertaken on 6th December 2016, 18th January 2017 and 13th February 2017 focusing on the area north of the radar. The preliminary results presented here should be considered with caution until further quality checks are performed. Between 6th December 2016 and 13th February 2017, considerable erosion was observed reaching up to 6 m of cliff face retreat and beach lowering of up to 0.5 m observed south of T1, while accretion (0.1 – 0.25 m) was observed to the north (Figure 17). Changes along four selected transects (T1 to T4, shown in Figure 17) indicate that cliff face retreat was more pronounced in T1 and T3, while beach lowering was observed along the four transects (Figure 18).

Cliff retreat was largest between 6th December 2016 and 18th January 2017 with little change between 18th January and 13th February 2017 (Figure 18) as already observed in beach changes described in Section 5. T3 showed the largest changes (reaching 6-7 m in the cliff top). At T4 cliff top changes were small but removal of talus from the cliff toe may increase the cliff face vulnerability to change. Steepening of the cliff face at T2 and T4 indicate they may be more vulnerable to cliff top retreat, while T1 and T3 are relatively protected (temporarily) by cliff toe talus.

These observations are comparable to the trends outlined in section 5 with largest changes observed between 6th December 2016 and 19th January 2017 and although the wave climate between 19th January and 13th February was comparable it is shown to have a smaller impact on the cliff and beach. This is likely due to the incidence time of peak wave height and tidal elevation but requires further analysis.

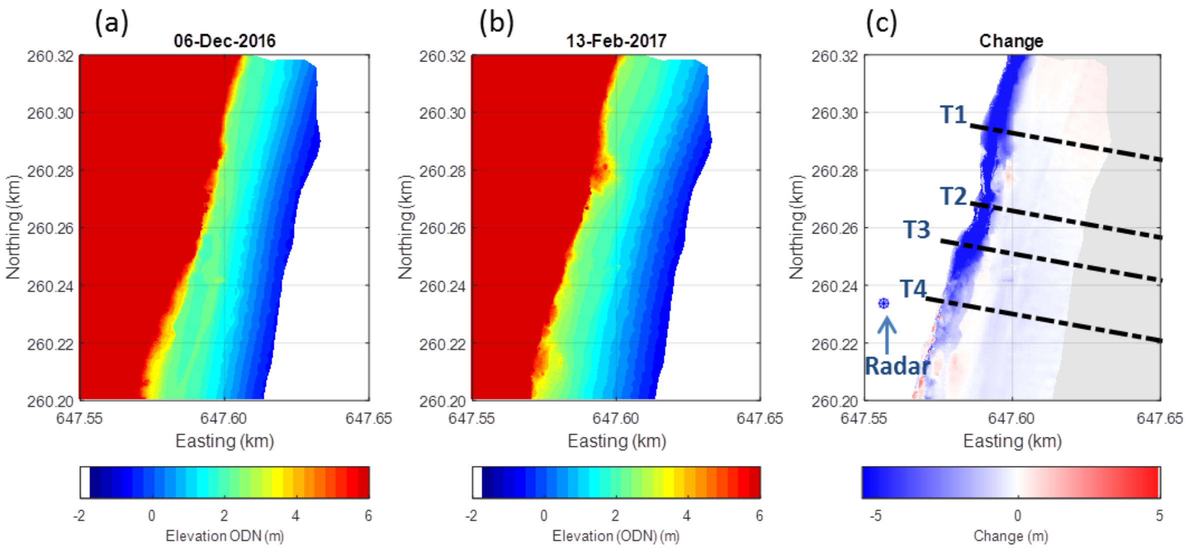

Figure 17. Beach elevation based on surveys conducted on 6th Dec 2016 (a) and 13th Feb 2017 (b) (represented at 0.1 m resolution) and the change between these surveys (c). Changes are arbitrarily constrained within ±5 m to reduce outliers. Cliff top elevations higher than 12 m were not resolved by the laser surveys.

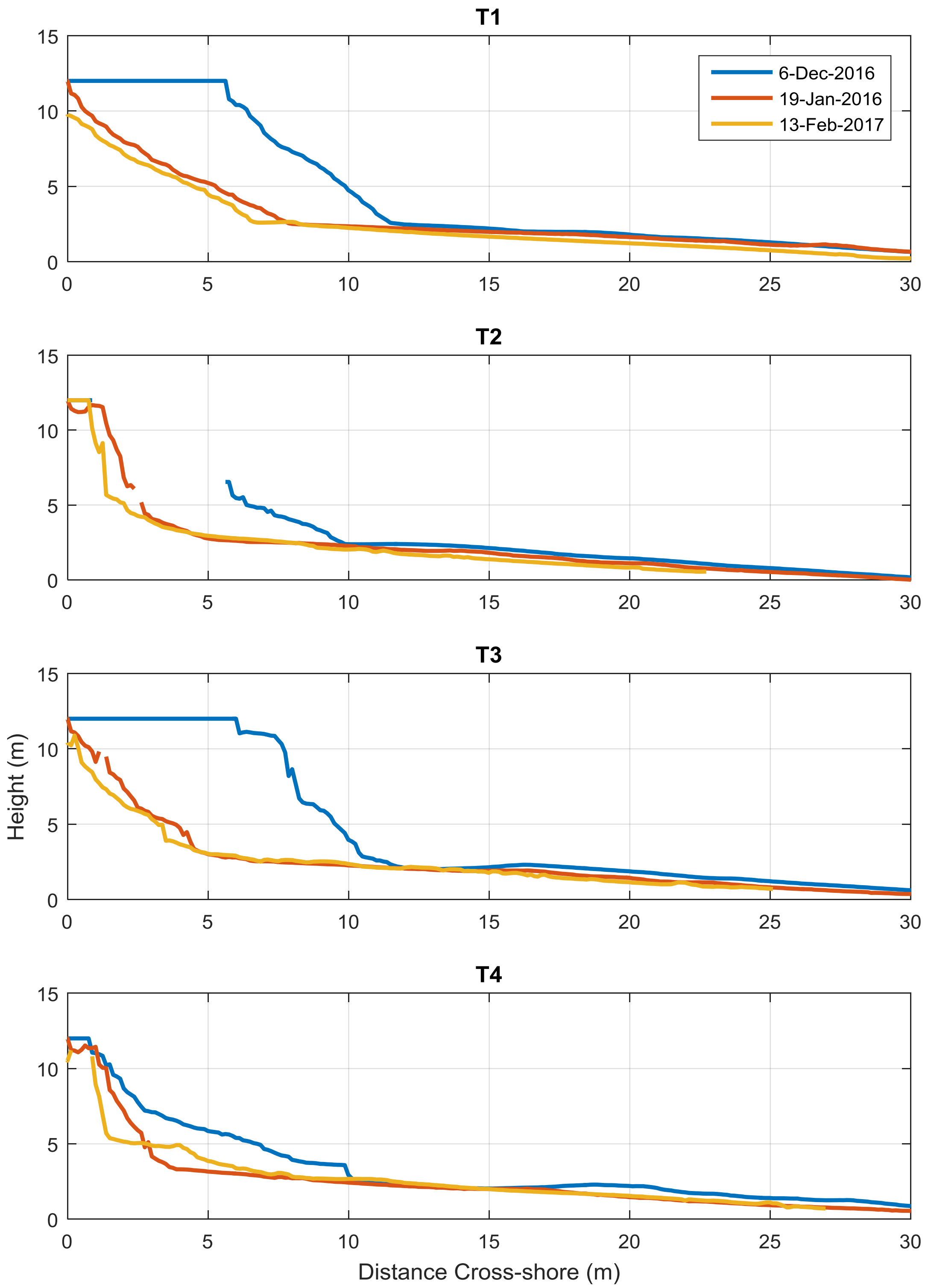

Figure 18. Elevation changes at four selected transects (T1-T4) between 6th Dec 2016 and 13th Feb 2017.

7 Research Plan and Future Steps

Progress report 3 will combine the analysis of nearshore bathymetric changes with beach changes to identify possible links between erosion and accretion patterns in relation to metocean conditions. Appropriate quality checks and assessment of suitability of data analysis methods will inform the results.

Further surveys are planned for the dates 27th–28th June 2017, 27th – 28th September 2017, January and April 2018 with possibility to undertake pre- and post-storm surveys dependent on forecast of significant events and availability of equipment. Processing of radar data is expected to be completed by July 2017. **Error! Not a valid bookmark self-reference.** provides an updated Gantt Chart for the work tasks and milestones.

Table 4. Gantt chart of research plan until completion of PhD.

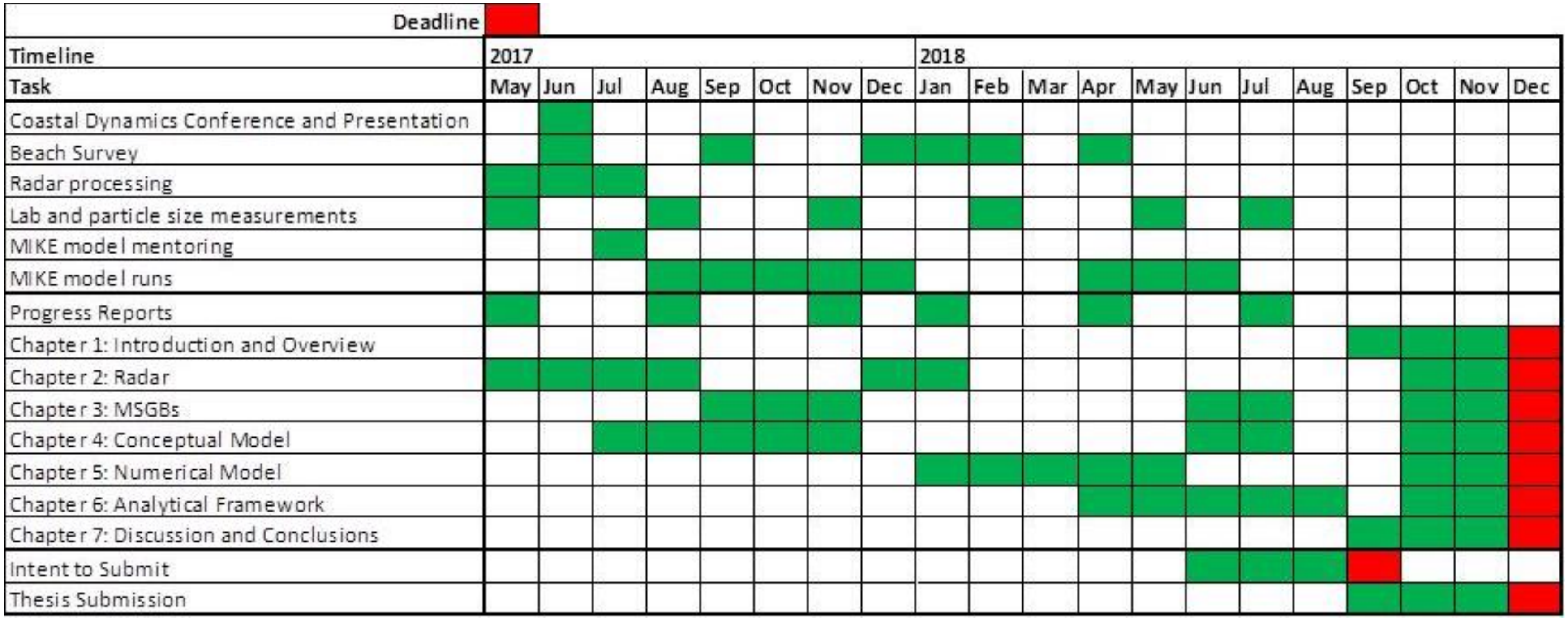

8 REFERENCES

Alpers, W. and Hassellmann, K., 1982, Spectral signal to clutter and thermal noise properties of ocean wave imaging synthetic aperture radars. International Journal of Remote Sensing, (3), 423–446

Borge, J. C. N., Reichert, K. and Dittmer, J., 1999. Use of nautical radar as a wave monitoring instrument. *Coastal Engineering*, 37 (3–4), 331–342.

Carrasco, R., Streßer, M., and Horstmann, J., 2016. A Simple Method for Retrieving Significant Wave Height from Dopplerized X-Band Radar. *Ocean Science Discussions* [online], (May), 1–14. Available from: http://www.ocean-sci-discuss.net/os-2016-29/.

Hessner, K., Wallbridge, S., and Dolphin, T., 2015. Validation of Areal Wave and Current Measurements Based on X-Band Radar, Technical note: 978-1-4799-8419-0/15 IEEE.

Izquierdo, P. and Guedes Soares, C., 2005. Analysis of sea waves and wind from X-band radar. *Ocean Engineering*, 32 (11–12), 1404–1419.

Reichert, K. and Lund, B., 2007. Ground based remote sensing as a tool to measure spatial wave field variations in coastal approaches. *Journal of Coastal Research, Proceedings of the 9th International Coastal Symposium* [online], 2007 (50).